Tectonophysics 619–620 (2014) 79–85

Contents lists available at ScienceDirect

Tectonophysics

journal homepage: www.elsevier.com/locate/tecto

Isotope geochemistry of mercury and its relation to earthquake in the Wenchuan Earthquake Fault Scientific Drilling Project Hole-1 (WFSD-1)

Lei Zhang [a,b], Yaowei Liu [a,*], Lishuang Guo [a], Duoxing Yang [a], Zhen Fang [c], Tao Chen [a], Hongwei Ren [a], Ben Yu [d]

[a] Key Laboratory of Crustal Dynamics, Institute of Crustal Dynamics, China Earthquake Administration, No.1, Anningzhuang Road, Beijing 100085, China
[b] Institute of Geophysics, China Earthquake Administration, Beijing 100081, China
[c] Anhui Earthquake Administration, Hefei 230031, China
[d] State Key Laboratory of Environmental Geochemistry, Institute of Geochemistry, Chinese Academy of Sciences, Guiyang 550002, China

ARTICLE INFO

Article history:
Received 7 January 2013
Received in revised form 26 July 2013
Accepted 19 August 2013
Available online 24 August 2013

Keywords:
Mercury
Mercury isotope ratios
Wenchuan earthquake
Rock cores
Wenchuan Earthquake Fault Scientific Drilling Project (WFSD)

ABSTRACT

Based on the Wenchuan Earthquake Fault Scientific Drilling Project (WFSD), we first investigated the distribution of the total mercury (THg) from 600 m to 1035 m of WFSD Hole-1 core (WFSD-1). The concentrations of THg in the fault gouge are significantly higher than in the sandstone, shale, siltstone, and cataclasite in WFSD-1. The THg concentrations in the main seismic fault zone range from 9.9 to 73.5 ng/g while those under the main fault range from 20.5 to 36 ng/g. To determine the source of Hg, typical rocks from different depths were chosen for Hg isotope analysis. The results show that δ^{202}Hg in the main seismic fault zone range from −0.11‰ to −2.68‰, and, below the seismic fault zone, δ^{202}Hg are from −0.64‰ to −1.33‰. The seismic fault rocks are more enriched in THg and have a larger variation of δ^{202}Hg compared to the other rocks. Mercury has different isotopic compositions and fractionation mechanisms in the fault zone, which are mainly affected by the earthquake and the fluid. The mercury isotope compositions reflect the fluid activities at the main fault zone. We demonstrate that mercury stable isotope ratios could serve as an effective tool for tracing mercury sources and monitoring and predicting earthquakes.

1. Introduction

Mercury (Hg) is an element which can be easily enriched in faults due to its special physical and chemical properties (Jin et al., 1989). Hg can migrate from depth to surface along a fault or rock fracture due to fluid carrying or a pressure gradient (Jin et al., 1989). Hg is widely used in earthquake monitoring, prediction and active fault detection in China (Liu, 2006; Tang et al., 2004). For example, anomalous Hg in wells or springs has been linked to earthquakes (Zhang et al., 2005); gas Hg concentration in the soil has been used to detect buried active faults (Wang et al., 2004). As an effective tool for tracing deep fluid activity (Stoffers et al., 1999), Hg plays an important role in revealing the relation between fluid activity in fault zone and mechanisms of strong earthquake preparation.

With the progress of analysis technology in recent years, the isotopic measurement technology has rapidly developed. For example, the wide use of multiple collector inductively coupled plasma mass spectrometry (MC-ICP-MS) has made it possible to measure mercury isotope composition precisely (Hintelmann and Lu, 2003; Lauretta et al., 2001; Xie et al., 2005; Yin et al., 2010a). Mercury is a volatile and biological activity element with strong redox properties, which may enhance the bacterial methylation processes that convert inorganic Hg to Me−Hg in the anoxic condition of sediment (Mason et al., 2006). The Hg isotope fractionation can be detected in the process of its transformation, such as chemical and microbial reduction, methylation, evaporation and condensation (Chen et al., 2012). Previous studies have demonstrated that Hg isotopes have both mass-dependent fractionation (MDF) and mass-independent fractionation (MIF) in biochemical and geochemical processes (Bergquist and Blum, 2007, 2009). MDF of Hg exists in the underground hydrothermal activity and smelting of ore, which could be used to trace the sources of mercury pollution, such as mines and smelters (Smith et al., 2005; Yin et al., 2013). The MIF may be related to the nuclear volume effect (NVE) (Schauble, 2007) and/or the magnetic isotope effect (MIE) (Buchachenko et al., 2004) with the latter usually causing the higher odd Hg MIF. MIF exists in aquatic organisms (Bergquist and Blum, 2007), peat (Shi et al., 2011), sediments (Feng et al., 2010), hot springs (Sherman et al., 2009), coal (Biswas et al., 2008), lichens (Carignan et al., 2009), atmospheric precipitation (Chen et al., 2012), and arctic snow exposed to sunlight (Sherman et al., 2010).

Mercury isotopes have been widely used in tracing the sources and migrations of Hg. Feng et al. (2010) took advantage of Hg isotopes and the end-member mixing model to study the pollution sources of Hg in the sediments of two adjacent reservoirs and determined that the Hg mainly came from the soil eroded by the rivers. Liu et al. (2011) used a ternary model to distinguish the main source of sediment mercury and found that the industrial district, the city and the background area had significant differences among THg, δ^{202}Hg and Δ^{199}Hg. Thus, Hg

* Corresponding author. Tel.: +86 1062911045.
E-mail address: liuyw20080512@126.com (Y. Liu).

0040-1951/$ – see front matter © 2013 Elsevier B.V. All rights reserved.
http://dx.doi.org/10.1016/j.tecto.2013.08.025

isotopes have great potential to be used to identify sources of Hg and indicate mercury geochemical processes (Yin et al., 2010b).

The Longmen–Shan fault zone is the tectonic boundary between the Tibetan Plateau to the west and the Sichuan Basin to the southeast (Luo and Liu, 2010), where the Mw 7.9 Wenchuan Earthquake happened on May 12, 2008. The first hole (WFSD-1) of the Wenchuan earthquake Fault Scientific Drilling (WFSD) project was drilled 178 days after the earthquake in order to understand the fault mechanism and the physical and chemical characteristics of the rocks in the earthquake zone (Li et al., 2013). The drilling project of the earthquake fault zone has also been conducted worldwide to conduct comprehensive research on various subjects, such as the Japan Nojima Fault Probe Project, the Taiwan Chelungpu fault Drilling Project (TCDP), and the USA San Andreas Fault Project. The geochemical research of these drilling projects focuses mainly on fluid activities (Tagami and Murakami, 2007; Yamada et al., 2007), mineralization within the fault zone (Hashimoto et al., 2007), and responses of gas geochemical anomaly to remote earthquakes (Li et al., 2006).

Previous research on mercury and its isotopes mainly focuse on the ecology and the Earth's surface environment (Gehrke et al., 2011; Sherman et al., 2010). WFSD-1 provides us an opportunity to study the underground fault rocks of the Earth, and, for the first time, enables us to study the relationship between mercury and its isotopes in the fault zone and tectonic activity during the earthquake process, and whether the mercury isotopic characteristics in the different sections of the fault zone could be used to reveal the source of mercury and the processes of earthquake rupture.

This study aims to evaluate the potential of using Hg isotopes to discriminate earthquake-induced mercury anomalies from the natural signatures in rocks from WFSD and to explain the tectonic significance revealed by mercury isotopes.

2. Geologic setting

The Wenchuan earthquake epicenter is located at the Longmenshan fault zone, which is composed of three thrust faults, including the Maoxian–Wenchuan fault, Yingxiu–Beichuan fault and Pengxian–Guanxian fault (Li et al., 2013). These thrust faults have minor right-lateral strike-slip component. The Wenchuan Mw 7.9 earthquake mainly occurred along the Yingxiu–Beichuan fault (Ran et al., 2010). The first hole of the Wenchuan earthquake Fault Scientific Drilling (WFSD-1) is located at Hongkou (Dujiangyan, Sichuan), which is 385 m away from the Hongkou earthquake surface rupture in the southern part of the Beichuan–Yingxiu fault zone (Fig. 1). This area is the major fault zone of the Wenchuan earthquake, and the surface rupture is obvious with the largest vertical movement of approximately 6 m (Zhang et al., 2010). The WFSD-1 hole with a depth of 1201.15 m was started on November 6, 2008 and finished on July 12, 2009. The drill hole above 590 m is composed of the Neoproterozoic Pengguan granite complex, which consists of the volcanic and granitoid rocks formed at 700–800 Ma. Below the depth of 590 m, the drill hole is composed of Late Triassic sedimentary rocks dominated by sandstone, siltstone, breccias and coal shales (Fig. 1). At the depth of 585.2 m, the drill hole intersects the main rupture plane of the Beichuan–Yingxiu fault, and there are at least 12 fault zones from 585.2 m to 693.37 m (Chen et al., 2011; Li et al., 2013). Li et al. (2013) found a 7 m-thick black fault gouge from 586 m to 593 m, which contains breccia, siltstone and charcoal shale. This thick fault gouge layer is the record of countless earthquake movements. At the same time, there are more than 20 ancient earthquake fault zones, which are more than 10 m in length with different attitudes and scales (Li et al., 2013). More detailed information about WFSD-1 can be found in Li et al. (2013). The core described in this study is from 600 m to 1035 m in depth.

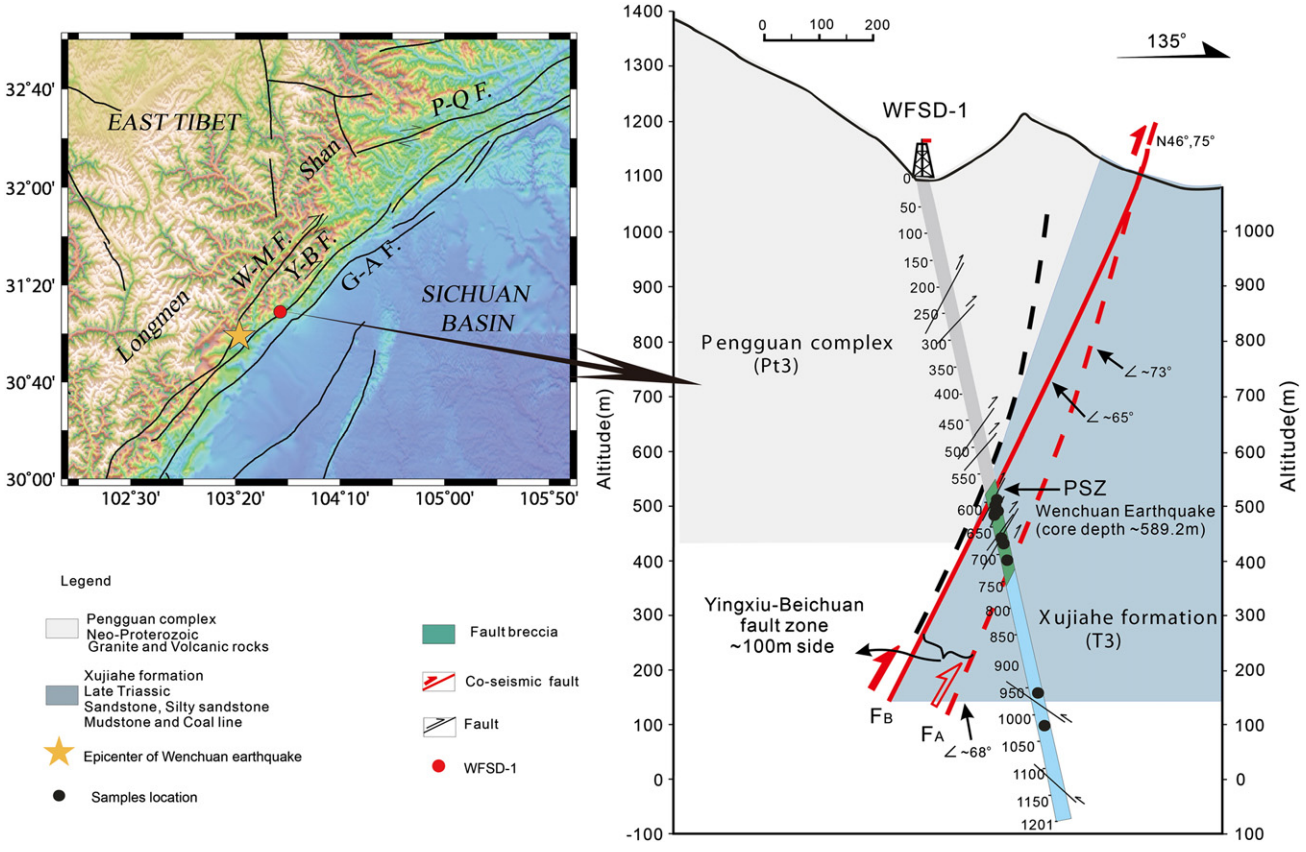

Fig. 1. Map of the 2008 Wenchuan earthquake geological structures and geologic cross-section across the WFSD-1 drilling site (modify from Li et al., 2013). W-MF.: Wenchuan–Maoxian Fault; Y-B F.: Yingxiu–Beichuan Fault; G-A F.: Guanxian–Anxian Fault; P-Q F.: Pingwu–Qingchuan Fault. PSZ: Principle Slip Zone. FA, FB: co-seismic fault, see Li et al. (2013) for details.

3. Sampling and analytical methods

3.1. Sampling and sample processing

The samples were collected from the Wenchuan Earthquake Fault Scientific Drilling Project Center. The general samples were stored in the dark sample library. The fault gouge samples were stored in the refrigerator. All samples were collected from the inner part of the cores and stored in sealed polyethylene bags to avoid any contamination during sampling. After air dried, homogenization, and milling, the samples were ground to sub-minus 200 mesh (≤75 μm) for total mercury (THg) and the Hg isotopic ratios analysis. The total Hg (THg) and Hg isotopic ratios were determined at the State Key Laboratory of Environmental Geochemistry, Institute of Geochemistry, Chinese Academy of Sciences, China.

The dried samples were digested in a water bath (95 °C) for a period of approximately 30 minutes with a mixture of HCl/HNO_3 (3:1, v/v). This digestion is necessary to keep the acid concentration below 20% (v/v), above which matrix interferences affect mercury isotopic measurements. The mass of digested samples was diluted with 18 MΩ water (Milli-Q) to a final mercury concentration of ~5 μg/L for isotope measurements (Yin et al., 2010a). All acids used in this work were guaranteed grade (HCl and HNO_3).

3.2. Total mercury analysis

The THg concentrations in WFSD-1 were analyzed for the dried samples using a Lumex RA 915$^+$ Hg analyzer equipped with a two-chamber pyrolysis block (Lumex Ltd., Russia). The processes were detailed by Rodriguez et al. (2007) and Liu et al. (2011). Briefly, the 200 mesh samples were heated to 800 °C in a first heating chamber, leading to the volatilization of the Hg and organic compounds of the sample. All products were transported from the first chamber to a second one by an air flow. The second chamber was continuously heated at about 800 °C. There, smoke and interference compounds were burnt, producing mostly carbon dioxide and water. Hg in the gas flow was determined by flameless atomic absorption spectrometry. A Zeeman corrector of the spectrometer eliminated the rest of the background absorption. All samples were checked at least twice, and the relative error of Lumex RA 915+ Hg analyzer was less than 10%. The detection limit for THg was 0.5 ng/g. Quality control was exercised by using method blanks and certified reference materials (GBW 07304a, IGGEC, Institute of Geophysical and Geochemical Exploration, China). The THg recovery for GBW 07304a was in the range of 93% to 109%.

3.3. Mercury isotope analysis

The Hg isotopic ratios were determined by MC-ICP-MS using a Nu-Plasma mass spectrometer equipped with twelve Faraday cups (Nu Instruments, Great Britain). A continuous flow cold-vapor generation system (CV) (HGX-200, CETAC U.S.) was coupled to an Apex-Q desolvation unit (Elemental Scientific Inc., U.S.) for Hg and Tl introduction, respectively. $SnCl_2$ solution which was purged of Hg with Hg-free N_2 was used as reducing agent and mixed online with Hg standards or sample digests to generate volatile elemental Hg. A typical sequence consisted of measuring the NIST SRM 3133 Hg solution before and after each sample (Liu et al., 2011). Instrument blanks were analyzed after each sample and each bracketing standard and on-line subtracted. Typical blank values were 10 mV for ^{202}Hg and 30 mV for ^{205}Tl, insignificant relative to typical sample and standard signals of 1 V for ^{202}Hg and 3 V for ^{205}Tl. A more detailed description of the sample pre-treatment method, the instrumental setup, the parameters, and the analytical conditions used in this study can be found in Yin et al. (2010a) and Liu et al. (2011).

The mass-dependent Hg isotope compositions are reported as δ^{xxx}Hg in permil (‰), referenced to NIST-3133, and are calculated as

$$\delta^{xxx}Hg\,‰ = 1000 \times \left[{}^{xxx}Hg/{}^{198}Hg_{\,unknown} / {}^{xxx}Hg/{}^{198}Hg_{\,NIST\ SRM\ 3133} - 1 \right] \quad (1)$$

The mass independent Hg isotope fractionations are reported as Δ^{xxx}Hg in permil (‰) and are calculated as below (Blum and Bergquist, 2007)

$$\Delta^{199}Hg\,‰ = \delta^{199}Hg - 0.252 \times \delta^{202}Hg \quad (2)$$

$$\Delta^{200}Hg\,‰ = \delta^{200}Hg - 0.502 \times \delta^{200}Hg \quad (3)$$

$$\Delta^{201}Hg\,‰ = \delta^{201}Hg - 0.752 \times \delta^{202}Hg \quad (4)$$

where XXX represents 202, 201, 200 and 199, respectively.

Reproducibility of the isotopic data was assessed by measuring replicate sample digests (typically between 2 and 4). Isotopic data of standard UM-Almadén with respect to the standard NIST 3133 were also measured the same way as other samples in each analytical session. The uncertainty of δ and Δ values for all UM-Almadén measurements were less than 0.1‰ and overall average were in agreement with published values (Blum and Bergquist, 2007). Uncertainties presented in the figures and tables in this paper correspond to the larger value of either 1) 2 SD of measurements of replicate sample digests, or 2) 2 SD of repeated measurements of the same digest at different analysis sessions.

4. Results

4.1. Total Mercury

The concentrations of the total Hg (THg) (Table 1) range from 9.9 ng/g at 671 m to 73.5 ng/g at 608 m, where the maximum THg is from the fault gouge and the minimum THg is from siltstone. The average concentration of sedimentary rocks (shale, siltstone and sandstone) is 17.8 ng/g. The average concentrations of the fault gouge and

Table 1
Total mercury concentrations and mercury isotopic compositions of rocks in WFSD-1.

Sample	Lithology	Depth/m	THg	δ^{199}Hg	2SD	δ^{200}Hg	2SD	δ^{201}Hg	2SD	δ^{202}Hg	2SD	Δ^{199}Hg	2SD	Δ^{200}Hg	2SD	Δ^{201}Hg	2SD
			ng/g	‰	‰	‰	‰	‰	‰	‰	‰	‰	‰	‰	‰	‰	‰
1	Sandstone	604	12.5	−0.20	0.06	−0.32	0.03	−0.42	0.05	−0.59	0.01	−0.05	0.07	−0.02	0.03	0.02	0.04
2	Fault gouge	608	73.5	−0.13	0.06	−0.14	0.03	−0.11	0.05	−0.11	0.01	−0.10	0.07	−0.09	0.03	−0.03	0.04
3	Shale	612	10.1	−0.15	0.11	−0.10	0.08	−0.24	0.04	−0.21	0.06	−0.10	0.10	0.01	0.05	−0.08	0.04
4	Fault gouge	618	60	−0.57	0.06	−1.33	0.04	−2.07	0.04	−2.68	0.04	0.11	0.05	0.02	0.02	−0.06	0.07
5	Siltstone	671	9.9	−0.69	0.06	−1.29	0.06	−1.71	0.01	−2.34	0.08	−0.10	0.04	−0.11	0.02	0.05	0.05
6	Cataclasite	680	44	−0.38	0.03	−0.51	0.04	−0.80	0.02	−0.92	0.04	−0.15	0.04	−0.05	0.03	−0.10	0.02
7	Cataclasite	711	27	−0.33	0.04	−0.61	0.003	−0.91	0.11	−1.33	0.07	0.01	0.06	0.06	0.04	0.09	0.05
8	Sandstone	966	36	−0.31	0.06	−0.61	0.02	−0.89	0.07	−1.21	0.06	−0.01	0.06	0.0004	0.03	0.02	0.03
9	Sandstone	1035	20.5	−0.20	0.07	−0.35	0.05	−0.45	0.04	−0.64	0.05	−0.04	0.06	−0.03	0.02	0.03	0.003

cataclasite are 51.13 ng/g, which is larger than those of sedimentary rocks.

4.2. Mercury isotopic compositions

The δ^{202}Hg values of the rocks in WFSD-1 range from −2.68‰ to −0.11‰, which are slightly lower than that of the gases at Volcano Island (−1.74‰ to −0.11‰; Zambardi et al., 2009), the hydrocarbon source rocks (−1.2‰ to 0.2‰) and sinters (−1.56‰ to −0.98‰) (Smith et al., 2008), but are close to coal (−0.11‰ to −2.98‰) (Feng et al., 2012). In the seismic main fault (600 m to 700 m), the δ^{202}Hg values are characterized by large variations (−2.68‰ to −0.11‰). However, the δ^{202}Hg values at 700 m to 1035 m are relatively stable compared with those of the main seismic fault (Fig. 2). The fault gouge at 618 m is isotopic lighter (δ^{202}Hg = −2.68‰) and has a positive Δ^{199}Hg (0.11‰).

Fig. 3 shows three isotope plots of δ^{199}Hg vs. δ^{202}Hg and δ^{201}Hg vs. δ^{202}Hg. These plots show obvious differences of rock samples from different depths, suggesting Hg isotopes undergo different fractionation processes. Moreover, the plots suggest that the Hg values of fault gouge at depths of 608 m and 618 m are affected mainly by earthquake processes, although they are not in the same area of the MDF line (Fig. 3). The isotope values between 608 m and 618 m show that the sources of Hg are different, which may be due to the deep fluids, the mercury phase transition (Hg^0 and Hg^{2+}) under high temperature, and/or several earthquakes.

Mass independent isotope fractionation (MIF) is observed in the rock samples from the main seismic fault (600 m to 680 m, Δ^{199}Hg = −0.15‰ to 0.11‰). No statistically significant MIF (Δ^{199}Hg = −0.04‰ to 0.01‰) is observed in any of the rock samples from 711 m to 1035 m, as shown in Table 1. MIF has been previously documented extensively in the surface environment (Das et al., 2013), but now is also observed in rock samples from borehole WFSD-1. There are two competing hypotheses for MIF fractionation including NVE and MIE. MIF due to NVE will evolve with a Δ^{199}Hg/Δ^{201}Hg ratio between 1.65 and 2.7 (Sonke, 2011). By contrast, MIF due to MIE will have slope of Δ^{199}Hg/Δ^{201}Hg close to unity (Das et al., 2013). In the WFSD-1 core samples, the Δ^{199}Hg/Δ^{201}Hg slope is 0.26 ± 0.50 and did not show any clear trends for Δ^{199}Hg/Δ^{201}Hg, which is due to the relatively small variation around zero for both ratios.

Fig. 4 shows δ^{202}Hg vs. Δ^{199}Hg of the rock samples. The isotopic fractionation in fault gouge is distinct from the other layers in WFSD-1. The Hg in the fault gouge, the sandstone, the shale, the siltstone and the cataclasite have different sources. Therefore, the mercury ranging from 680 m to 1035 m are due to background values, and the sources of mercury and isotope fractionation in the main seismic fault are affected by the earthquake.

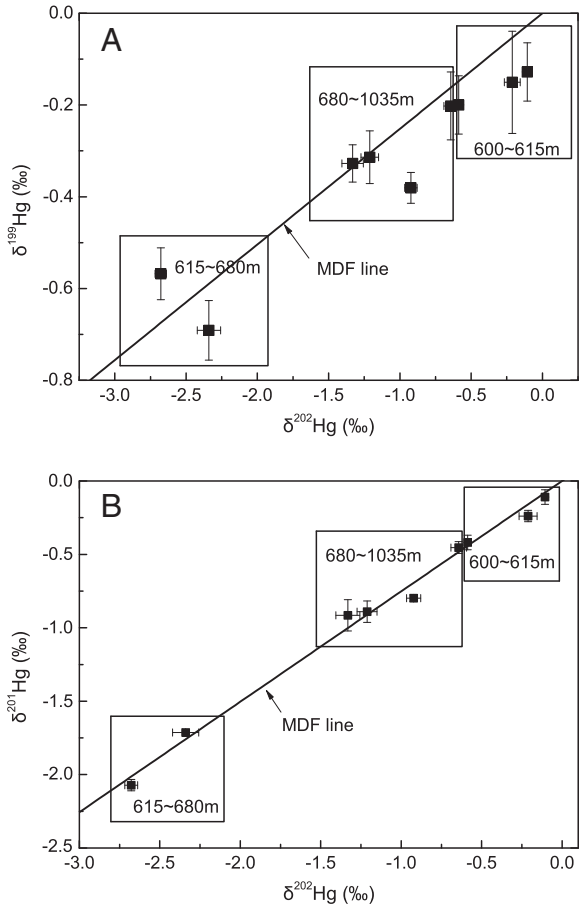

Fig. 3. Three-isotope plots of δ^{199}Hg vs. δ^{202}Hg (A) and δ^{201}Hg vs. δ^{202}Hg (B) of all samples. The isotopic compositions are reported per mil (‰) relative to the Hg standard NIST 3133. The solid line represents the theoretical mass-dependent fractionation line based on the exponential law (Blum and Bergquist, 2007) and using δ^{199}Hg = 0.252 × δ^{202}Hg and δ^{201}Hg = 0.752 × δ^{202}Hg.

5. Discussion

5.1. Indication of THg and Hg isotopes

Clay minerals absorb Hg in sediment (Yan et al., 2008), and the fault gouges are rich in clay minerals (Buatier et al., 2012; Kuo et al., 2009). The fault gouges in Hongkou outcrop which are ~385 m near the

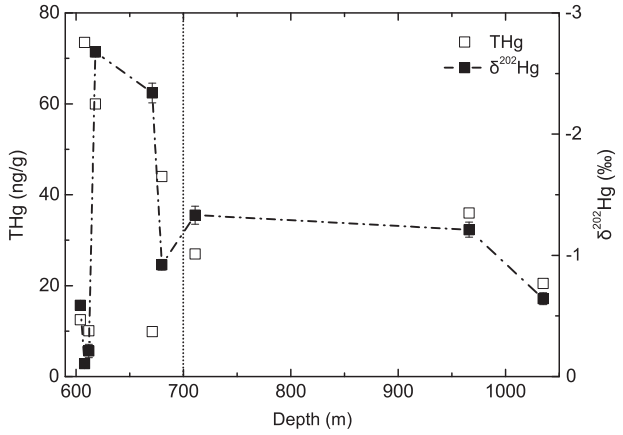

Fig. 2. Variations of the total Hg concentrations and δ^{202}Hg vs. depth in the rocks taken from WFSD-1. Note that the δ^{202}Hg values broadly correlate with THg with the negative δ^{202}Hg recorded in high Hg concentrations.

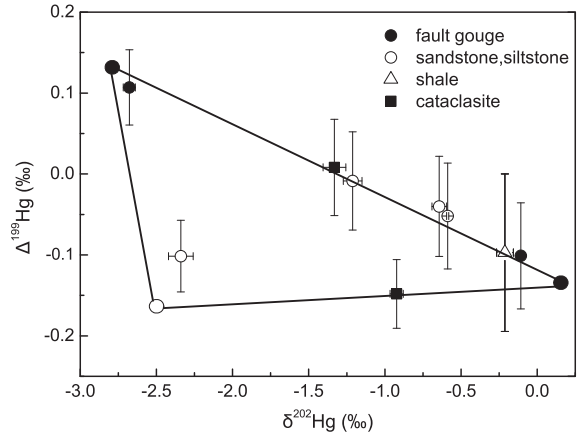

Fig. 4. δ^{202}Hg vs. Δ^{199}Hg of rocks samples from WFSD-1. The three lines represent the rough variations of the Hg isotope values. The combination of MDF/MIF signatures of the rocks indicate a complex mixing Hg sources.

WFSD-1, are relatively rich in clay minerals, with total clay contents of ~43% (wt.%), and the major minerals in the gouges are quartz, calcite and dolomite, with total contents of carbonates of ~18% (Zhang and He, 2013). The high THg in fault gouges are probably due to the high content of clay minerals, which tend to enrich mercury. The high THg in cataclasites are due to the fractured surface, which enhanced surface adsorption of Hg. The fault gouge and cataclasite are formed due to the process of earthquake. The high THg concentrations of the fault rocks are thus related to earthquake. The adsorption of Hg in fault rocks is a complex process, which changed the physical-chemical of fault rocks, such as clay minerals, organic matter and crack density. These results indicate that seismic activity prompted the absorption and accumulation of Hg.

The δ^{202}Hg has a larger variation (−2.68‰ to −0.11‰) between 600 m and 700 m, which is the main fault of the Wenchuan earthquake. It suggests that there is fractionation of mercury isotopes within this depth range. The main fault have lower δ^{202}Hg values at 618 m (δ^{202}Hg = −2.68‰, fault gouge) and 671 m (δ^{202}Hg = −2.34‰, siltstone) than at other depths (Fig. 3). The ^{202}Hg depletion may be due to the fluid activity (fluid migration, volatilization, boiling and water–rock reactions, etc.) during the earthquake. The Hg is derived from the surrounding rock under high temperature and dissolved in fluid ($Hg^0_{(aq)}$), $Hg^0_{(aq)}$ in the fluid can be volatilized to $Hg^0_{(g)}$ (Smith et al., 2005, 2008). These combined effects are confirmed to produce a vapor/liquid containing light Hg isotopes (Smith et al., 2005, 2008).

5.2. Factors affecting mercury fractionation in the fault zones

Many processes, such as deep fluid activity (Smith et al., 2005), photo-oxidation (Zheng et al., 2007) and the re-emission of mercury (Farmer et al., 2009), can induce the fractionation of mercury isotopes in natural environmental, but their relative contributions are not fully characterized (Shi et al., 2011).

It is difficult to determine which process is dominant for the mercury isotope fractionation in rocks of this study. However, our results clearly indicate that earthquake-induced Hg isotopic fractionation is distinct from that induced by the normal sedimentary environment. During the earthquakes, mercury anomalies can be caused by the reaction of rocks with deep-sourced Hg carried up by the deep fluid. In addition, the Hg anomalies can be induced by the phase transformation of Hg due to the high temperature and pressure prompted by the earthquake (Wang et al., 1991). By contrast, the natural sources release mercury gradually in normal sedimentary environments and geothermal gradients. The emission of Hg in natural processes is slow and mainly driven by the reduction of Hg^{2+} to Hg^0 through microbiological, chemical and photochemical processes (Lindberg et al., 2007). However, the emission of mercury from earthquake-induced sources is a rapid discharge and is accumulated in the fractured rock, which is controlled by the thermal reduction of Hg^{2+} at high temperatures (Shi et al., 2011). The different mercury formation mechanisms result in different isotopic compositions.

The fault gouge is formed when rocks are repeatedly crushed and fractured in a fault zone over a long period of time, which carries information on fault activities (Fu et al., 2008). In other words, the fault gouge is a production of the seismic event (Ma et al., 2006). The mercury isotope ratios of two fault gouge samples show quite different signature (Fig. 3; Table 1). Seismic intensity, lithology of wall rocks (Li et al., 2013), and rock–fluid interactions (Fu et al., 2008) can all affect the fault gouge compositions. Li et al. (2013) has found that the crack density of rock cores at the depth of 608 m and 618 m are similar, which is nearly 25. The two fault gouge samples are both from Xujiahe Formation. The hanging wall rocks at the depth of 608 m and 618 m are both sandstone. However, the footwall rocks are sandstone and pelite, respectively. The sandstone and mudstone of the California Coast Ranges, USA, show δ^{202}Hg values of −0.53‰ to −1.21‰, and −0.27‰ to −0.93‰, respectively (Smith et al., 2008). The δ^{202}Hg value of sandstone from this study is −0.59‰ to −1.21‰, which is similar to the sandstone from California Coast Ranges (Smith et al., 2008).

In previous study, there is only one report investigated the typical crustal rocks, with δ^{202}Hg values of −0.60 ± 0.2‰ (1SD, n = 30) (Smith et al., 2008). δ^{202}Hg data of UM-Almadén, which from the largest industrial source of Hg, has the δ^{202}Hg value of −0.54‰ (Blum and Bergquist, 2007), falling within the range of rock samples (Bergquist and Blum, 2009; Smith et al., 2008). However, the δ^{202}Hg values of two fault gouge samples are −0.11‰ and −2.68‰, which have a wide range of variation and are quite different from other rocks in this study and Smith et al. (2008). The different δ^{202}Hg values of fault gouge may be due to earthquake. The fault gouge is formed under high temperature (Kuo et al., 2011). Ishikawa et al. (2008) found that there were high-temperature fluids (>350 °C) at fault gouge zone during the 1999 magnitude 7.6 Chi–Chi earthquake along the Chelungpu fault. Lei et al. (2009) found there existed fluid within the Longmenshan fault zone, which may affect the occurrence of the large Wenchuan earthquake. The water content of fault gouge at the depth of 608 m is low, while it is higher at the depth of 618 m (Li et al., 2013). So there may be fluid-riched surroundings at the depth of 618 m. Therefore, we infer that there are also high-temperature fluids in the fault gouge of WFSD-1 during the earthquake, and the fractionation of Hg may relate to the hydrothermal systems. Smith et al. (2008) found that isotopic fractionation took place during transport and/or deposition Hg, and redox transformations led to Hg isotope fractionation in hydrothermal systems in the California Coast Range. The boiling of hydrothermal fluids is one of the most important processes that causing the Hg isotope fractionation (Smith et al., 2005, 2008). Recent laboratory experiments show that a maximum δ^{202}Hg fractionation of 1‰ is caused by the volatilization of $Hg^0_{(aq)}$ (Zheng et al., 2007). Smith et al. (2005) found that δ^{202}Hg values of veins/fault 290 m and 275 m below the sinter of a fossil hydrothermal system were −1.4‰ to 1.3‰. There is 5‰ variations of δ^{202}Hg values observed for epithermal deposits, in which the isotopic fractionation is probably due to boiling of deep vein fluids. Other low-temperature deposits in which boiling is uncommon, have δ^{202}Hg values ranging from only 0.4‰ to −1.5‰ (UM-Almadén) and 0.0‰ to −1.3‰ (NIST SRM 1641d) (Hintelmann and Lu, 2003, Smith et al., 2005). The larger variation of Hg isotope value of fault gouge at 618 m indicates that its fractionation is affected by high temperature fluids and kinetic effects during earthquake. However, the fault gouge at 608 m was less affected by boiling fluids than that of 618 m, which induced minor fractionation. Of course, more data are needed to be discussed in details.

The THg at 671 m is low (9.9 ng/g) (Fig. 2). Chi (2004) has found that the concentration of mercury in siltstone (9.6 ng/g) is less than that of other sedimentary rocks in China. The lower Hg content at 671 m indicates that the concentration of Hg is the base value and there is less mercury in the surrounding environment than at other depths. However the δ^{202}Hg value at 671 m (−2.34‰) is close to that at 618 m (δ^{202}Hg = −2.68‰). Accordingly to the geological setting (Li et al., 2013), the borehole at the two depths are very similar with both in the Yingxiu–Beichuan fault zone. They have high water content, and wall rocks are pelite. There are cracks at 671 m and fault gouge at 618 m, indicating that the δ^{202}Hg fractionation mechanism at 671 m is similar to that of fault gouge at 618 m under the same geological setting.

6. Conclusions

Our research of the mercury isotopic compositions of the Wenchuan earthquake fault zone rocks lead to the following conclusions:

The THg values in the fault gouge (60 ng/g to 73.5 ng/g) are greater than those of other rocks (9.9 ng/g to 44 ng/g) in WFSD-1. The Hg isotopes of WFSD-1 reveal distinct MDF and MIF signatures between the main seismic fault rocks and the other rocks. The rocks in the seismic main fault have distinct Δ^{199}Hg. In contrast, the rocks below the seismic

fault have slightly negative to zero Δ^{199}Hg. Based on these results, we suggest that the Hg in the fault gouge is dominantly earthquake-induced. We suggest that the isotopic compositions largely reflect the Hg isotopic signal of the earthquake and fluid. Our data shows the simplest explanations of mercury sources (earthquakes or natural sources) have different isotopic compositions and fractionation mechanisms. This study explore the applicability of using mercury isotope ratio to trace mercury originated from earthquake.

Acknowledgements

This work was supported by the "Wenchuan Earthquake Fault Scientific Drilling" (WFSD-10) of the National Science and Technology Planning Project and the Research Grant from the Institute of Crustal Dynamics, CEA, under Contract No. ZDJ2012-07. We would like to thank Dr. X.B. Feng of the Institute of Geochemistry, Chinese Academy of Science, for his aid in the analysis. Anonymous reviewers and the Editor are thanked for their constructive comments that significantly improved the quality of the manuscript.

References

Bergquist, B.A., Blum, J.D., 2007. Mass-dependent and -independent fractionation of Hg isotopes by photoreduction in aquatic systems. Science 318 (5849), 417–420.
Bergquist, B.A., Blum, J.D., 2009. The odds and evens of mercury isotopes: applications of mass-dependent and mass-independent isotope fractionation. Elements 5 (6), 353–357.
Biswas, A., Blum, J.D., Bergquist, B.A., Keeler, G.J., Xie, Z., 2008. Natural mercury isotopes variation in coal deposits and organic soils. Environ. Sci. Technol. 42 (22), 8303–8309.
Blum, J.D., Bergquist, B.A., 2007. Reporting of variations in the natural isotopic composition of mercury. Anal. Bioanal. Chem. 388 (2), 353–359.
Buatier, M., Chauvet, A., Kanitpanyacharoen, W., Wenk, H.-R., Ritz, J.-F., Jolivet, M., 2012. Origin and behavior of clay minerals in the Bogd fault gouge, Mongolia. J. Struct. Geol. 34, 77–90.
Buchachenko, A.L., Kouznetsov, D.A., Shishkov, A.V., 2004. Spin biochemistry: magnetic isotope effect in the reaction of creatine kinase with CH_3HgCl. J. Phys. Chem. A 108 (5), 707–710.
Carignan, J., Estrade, N., Sonke, J.E., Donard, O.F.X., 2009. Odd isotope deficits in atmospheric Hg measured in lichens. Environ. Sci. Technol. 43 (15), 5660–5664.
Chen, Q., Qian, R.Y., Chang, S.L., Jiang, M., Zhang, G.B., 2011. Acquisition methods of 2D reflection seismic short profile through WFSD-1 in main faults of Wenchuan earthquake. Chin. J. Geophys. 54 (8), 2060–2071 (in Chinese with English abstract).
Chen, J.b, Hintelmann, H., Feng, X.B., Dimock, B., 2012. Unusual fractionation of both odd and even mercury isotopesin precipitation from Peterborough, ON, Canada. Geochim. Cosmochim. Acta 90, 33–46.
Chi, Q.H., 2004. Abundance of mercury in crust, rocks and loose sediments. Geochimica 33 (6), 641–648 (in Chinese with English abstract).
Das, R., Bizimis, M., Wilson, A.M., 2013. Tracing mercury seawater vs. atmospheric inputs in a pristine SE USA salt marsh system: mercury isotope evidence. Chem. Geol. 336, 50–61.
Farmer, J.G., Anderson, P., Cloy, J.M., Graham, M.C., MacKenzie, A.B., Cook, G.T., 2009. Historical accumulation rates of mercury in four Scottish ombrotrophic peat bogs over the past 2000 years. Sci. Total. Environ. 407 (21), 5578–5588.
Feng, X.B., Foucher, D., Hintelmann, H., Yan, H., He, T., Qiu, G., 2010. Tracing mercury contamination sources in sediments using mercury isotope compositions. Environ. Sci. Technol. 44 (9), 3363–3368.
Feng, X.B., Yin, R.S., Yu, B., Du, B., 2012. Mercury isotope variations in surface soils in different contaminated areas in Guizhou Province, China. Chin. Sci. Bull. 57. http://dx.doi.org/10.1007/s11434-012-5488-1.
Fu, B.H., Wang, P., Kong, P., Zheng, G.D., Wang, G., Shi, P.L., 2008. Preliminary study of coseismic fault gouge occurred in the slip zone of the Wenehuan Ms 8.0 earthquake and its tectonic implications. Acta Petrol. Sin. 24 (10), 2237–2243 (in Chinese with English abstract).
Gehrke, G.E., Blum, J.D., Marvin-DiPasquale, M., 2011. Sources of mercury to San Francisco Bay surface sediment as revealed by mercury stable isotopes. Geochim. Cosmochim. Acta 75 (3), 691–705.
Hashimoto, Y., Ujiie, K., Sakaguchi, A., Tanaka, H., 2007. Characteristics and implication of clay minerals in the northern and southern parts of the Chelung-pu fault, Taiwan. Tectonophysics 443, 233–242.
Hintelmann, H., Lu, S., 2003. High precision isotope ratio measurements of mercury isotopes in cinnabar ores using multicollector inductively coupled plasma mass spectrometry. Analyst 128, 635–639.
Ishikawa, T., Tanimizu, M., Nagaishi, K., Matsuoka, J., Tadai, O., Sakaguchi, M., Hirono, T., Mishima, T., Tanikawa, W., Lin, W., Kikuta, H., Soh, W., Song, S.R., 2008. Coseismic fluid–rock interactions at high temperatures in the Chelungpu fault. Nat. Geosci. 1, 679–683.
Jin, Y., Wu, Z., Shen, C., Wei, J., Zhu, H., 1989. Earthquake prediction through the observation and measurement of mercury content variation in water. J. Geochem. Explor. 33, 195–202.
Kuo, L.W., Song, S.R., Yeh, E.C., Chen, H.F., 2009. Clay mineral anomalies in the fault zone of the Chelungpu Fault, Taiwan, and their implications. Geophys. Res. Lett. 36 (L18306). http://dx.doi.org/10.1029/2009GL039269.
Kuo, L.-W., Song, S.-R., Huang, L., Yeh, E.-C., Chen, H.-F., 2011. Temperature estimates of coseismic heating in clay-rich fault gouges, the Chelungpu fault zones, Taiwan. Tectonophysics 502 (3), 315–327.
Lauretta, D.S., Klaue, B., Blum, J.D., Buseek, P.R., 2001. Mercury abundances and isotopic compositions in the Murchison(CM) and Allende (CV) carboneous chrondrites. Geochim. Cosmochim. Acta 65, 2807–2818.
Lei, J.S., Zhao, D.P., Su, J.R., Zhang, G.W., Li, F., 2009. Fine seismic structure under the Longmenshan fault zone and the mechanism of the large Wenchuan earthquake. Chin. J. Geophys. 52 (2), 339–345 (in Chinese with English abstract).
Li, S.Q., Sun, Q., Luo, L.Q., Zhan, X.C., 2006. Relationship between earthquake and the gas geochemical anomalies in the 0 2000 m mud of Chinese Continent Scientific Drilling hole. Acta Petrol. Sin. 22 (7), 2095–2102 (in Chinese with English abstract).
Li, H., Wang, H., Xu, Z., Si, J., Pei, J., Li, T., Huang, Y., Song, S.R., Kuo, L.W., Sun, Z., Chevalier, M.L., Liu, D., 2013. Characteristics of the fault-related rocks, fault zones and the principal slip zone in the Wenchuan Earthquake Fault Scientific Drilling Project Hole-1 (WFSD-1). Tectonophysics 584 (22), 23–42.
Lindberg, S., Bullock, R., Ebinghaus, R., Engstrom, D., Feng, X., Fitzgerald, W., Pirrone, N., Prestbo, E., Seigneur, C., 2007. A synthesis of progress and uncertainties in attributing the sources of mercury in deposition. Ambio 36 (1), 19–33.
Liu, Y., 2006. Review of the research progress on the seismological science of underground fluid in China during last 40 years. Earthquake Res. China 22 (3), 222–235 (in Chinese with English abstract).
Liu, J.L., Feng, X.B., Yin, R.S., Zhu, W., Li, Z.G., 2011. Mercury distributions and mercury isotope signatures in sediments of Dongjiang River, the Pearl River Delta, China. Chem. Geol. 287, 81–89.
Luo, G., Liu, M., 2010. Stress evolution and fault interactions before and after the 2008 Great Wenchuan earthquake. Tectonophysics 491, 127–140.
Ma, K.F., Tanaka, H., Song, S.R., Wang, C.Y., Hung, J.H., Tsai, Y.B., Mori, J., Song, Y.F., Yeh, E.C., Soh, W., Sone, H., Kuo, L.W., Wu, H.Y., 2006. Slip zone and energetics of a large earthquake from the Taiwan Chelungpu-fault Drilling Project. Nature 444, 473–476.
Mason, R.P., Kim, E.-H., Cornwell, J., Heyes, D., 2006. An examination of the factors influencing the flux of mercury, methylmercury and other constituents from estuarine sediment. Mar. Chem. 102, 96–110.
Ran, Y., Chen, L., Chen, J., Wang, H., Chen, G., Yin, J., Shi, X., Li, C., Xu, X., 2010. Paleoseismic evidence and repeat time of large earthquakes at three sites along the Longmenshan fault zone. Tectonophysics 491, 141–153.
Rodriguez, L., Rincon, J., Asencio, I., Rodriguez-Castellanos, L., 2007. Capability of selected crop plants for shoot mercury accumulation from polluted soils: Phytoremediation perspectives. Int. J. Phytoremediation 9, 1–13.
Schauble, E.A., 2007. Role of nuclear volume in driving equilibrium stable isotope fractionation of mercury, thallium, and other very heavy elements. Geochim. Cosmochim. Acta 71 (9), 2170–2189.
Sherman, L.S., Blum, J.D., Nordstrom, D.K., McCleskey, R.B., Barkay, T., Vetriani, C., 2009. Mercury isotopic composition of hydrothermal systems in the Yellowstone Plateau volcanic field and Guaymas Basin sea-floor rift. Earth Planet. Sci. Lett. 279 (1–2), 86–96.
Sherman, L.S., Blum, J.D., Johnson, K.P., Keeler, G.J., Barres, J.A., Douglas, T.A., 2010. Mass-independent fractionation of mercury isotopes in Arctic snow driven by sunlight. Nat. Geosci. 3, 173–177.
Shi, W.F., Feng, X.B., Zhang, G., Ming, L.L., Yin, R.S., Zhao, Z.Q., Wang, J., 2011. High-precision measurement of mercury isotope ratios of atmospheric deposition over the past 150 years recorded in a peat core taken from Hongyuan, Sichuan Province, China. Chin. Sci. Bull. 56 (9), 877–882.
Smith, C.N., Kesler, S.E., Klaue, B., Blum, J.D., 2005. Mercury isotope fractionation in fossil hydrothermal systems. Geology 33 (10), 825–828.
Smith, C.N., Kesler, S.E., Blum, J.D., Rytuba, J.J., 2008. Isotope geochemistry of mercury in source rocks, mineral deposits and spring deposits of the California Coast Ranges, USA. Earth Planet. Sci. Lett. 269, 399–407.
Sonke, J.E., 2011. A global model of mass independent mercury stable isotope fractionation. Geochim. Cosmochim. Acta 75 (16), 4577–4590.
Stoffers, P., Hannington, M., Wright, I., Herzig, P., de Ronde, C., 1999. Elemental mercury at submarine hydrothermal vents in the Bay of Plenty, Taupo volcanic zone, New Zealand. Geology 27 (10), 931–934.
Tagami, T., Murakami, M., 2007. Probing fault zone heterogeneity on the Nojima fault: Constraints from zircon fission-track analysis of borehole samples. Tectonophysics 443, 139–153.
Tang, C., Wang, Y., Fu, H., 2004. Characteristics of short-term synthetical anomalies of radon and mercury content in groundwater in Sichuan–Yunnan region before strong earthquakes. J. Seismol. Res. 27, 18–22 (in Chinese with English abstract).
Wang, C.M., Li, X.H., Wei, B.L., 1991. Applications of Measurement of Fracture Gases in Seismological Science. Earthquake Press, Beijing 22–30 (in Chinese).
Wang, C., Du, J., Zhou, X., 2004. Geochemical feature of mercury across Sanhe–Pinggu active fault. Earthquake 24 (1), 132–136 (in Chinese with English abstract).
Xie, Q.L., Lu, S.Y., Evans, D., Dillon, P., Hintelmann, H., 2005. High precision Hg isotope analysis of environmental samples using gold trap-MC-ICP-MS. J. Anal. At. Spectrom. 20, 515–522.
Yamada, R., Matsuda, T., Omura, K., 2007. Apatite and zircon fission-track dating from the Hirabayashi-NIED borehole, NojimaFault, Japan: Evidence for anomalous heating in fracture zones. Tectonophysics 443, 153–160.
Yan, H., Feng, X., Shang, L., Qiu, G., Dai, Q., Wang, S., Hou, Y., 2008. The variations of mercury in sediment profiles from a historically mercury-contaminated reservoir. Guizhou province, China. Sci. Total. Environ. 407, 497–506.
Yin, R.S., Feng, X.B., Foucher, D., Shi, W.F., Zhao, Z.Q., Wang, J., 2010a. High precision determination of mercury isotope ratios using online mercury vapor generation system

coupled with multi-collector inductively coupled plasma-mass spectrometer. Chin. J. Anal. Chem. 38 (7), 929–934 (in Chinese with English abstract).
Yin, R.S., Feng, X.B., Shi, W.F., 2010b. Application of the stable-isotope system to the study of sources and fate of Hg in the environment: A review. Appl. Geochem. 25, 1467–1477.
Yin, R.S., Feng, X.B., Wang, J.X., Li, P., Liu, J.L., Zhang, Y., Chen, J.B., Zheng, L.R., Hu, T.D., 2013. Mercury speciation and mercury isotope fractionation during ore roasting process and their implication to source identification of downstream sediment in the Wanshan mercury mining area, SW China. Chem. Geol. 336, 72–79.
Zambardi, T., Sonke, J.E., Toutain, J.P., Sortino, F., Shinohara, H., 2009. Mercury emissions and stable isotopic compositions at Vulcano Island (Italy). Earth Planet. Sci. Lett. 277, 236–243.
Zhang, L., He, C., 2013. Frictional properties of natural gouges from Longmenshan fault zone ruptured during the Wenchuan Mw 7.9 earthquake. Tectonophysics 594, 149–164.
Zhang, F.Q., Ren, J., Li, H.X., Zhang, Y.Q., Wang, X.J., 2005. Relationship between the anomalies of underground fluid in the Huailai NO.4 well and earthquake. Seismol. Geol. 27 (1), 123–130 (in Chinese with English abstract).
Zhang, P.Z., Wen, X.Z., Shen, Z.K., Chen, J.H., 2010. Oblique high-angle listric-reverse faulting and associated straining processes: the Wenchuan earthquake of 12 May 2008, Sichuan, China. Ann. Rev. Earth Planet. Sci. 38, 353–382.
Zheng, W., Foucher, D., Hintelmann, H., 2007. Mercury isotope fractionation during volatilization of Hg(0) from solution into the gas phase. J. Anal. At. Spectrom. 22, 1097–1104.